

## Discovery of (Thienopyrimidin-2-yl)aminopyrimidines as Potent, Selective, and Orally Available Pan-PI3-Kinase and Dual Pan-PI3-Kinase/mTOR Inhibitors for the Treatment of Cancer

Daniel P. Sutherland,<sup>\*,†</sup> Deepak Sampath,<sup>†</sup> Megan Berry,<sup>†</sup> Georgette Castanedo,<sup>†</sup> Zhigang Chang,<sup>†</sup> Irina Chuckowree,<sup>‡</sup> Jenna Dotson,<sup>†</sup> Adrian Folkes,<sup>‡</sup> Lori Friedman,<sup>†</sup> Richard Goldsmith,<sup>†</sup> Tim Heffron,<sup>†</sup> Leslie Lee,<sup>†</sup> John Lesnick,<sup>†</sup> Cristina Lewis,<sup>†</sup> Simon Mathieu,<sup>†</sup> Jim Nonomiya,<sup>†</sup> Alan Olivero,<sup>†</sup> Jodie Pang,<sup>†</sup> Wei Wei Prior,<sup>†</sup> Laurent Salphati,<sup>†</sup> Steve Sideris,<sup>†</sup> Qingping Tian,<sup>†</sup> Vickie Tsui,<sup>†</sup> Nan Chi Wan,<sup>‡</sup> Shumei Wang,<sup>†</sup> Christian Wiesmann,<sup>†</sup> Susan Wong,<sup>†</sup> and Bing-Yan Zhu<sup>†</sup>

<sup>†</sup>Genentech, Inc., 1 DNA Way, South San Francisco, California 94080 and <sup>‡</sup>Piramed Pharma, 957 Buckingham Avenue, Slough, Berks SL1 4NL, United Kingdom

Received August 27, 2009

The PI3K/AKT/mTOR pathway has been shown to play an important role in cancer. Starting with compounds **1** and **2** (GDC-0941) as templates, (thienopyrimidin-2-yl)aminopyrimidines were discovered as potent inhibitors of PI3K or both PI3K and mTOR. Structural information derived from PI3K $\gamma$ -ligand cocrystal structures of **1** and **2** were used to design inhibitors that maintained potency for PI3K yet improved metabolic stability and oral bioavailability relative to **1**. The addition of a single methyl group to the optimized **5** resulted in **21**, which had significantly reduced potency for mTOR. The lead compounds **5** (GNE-493) and **21** (GNE-490) have good pharmacokinetic (PK) parameters, are highly selective, demonstrate knock down of pathway markers in vivo, and are efficacious in xenograft models where the PI3K pathway is deregulated. Both compounds were compared in a PI3K $\alpha$  mutated MCF7.1 xenograft model and were found to have equivalent efficacy when normalized for exposure.

### Introduction

The PI3K/Akt/mTOR<sup>a</sup> pathway plays a central role in cell proliferation, migration, survival, and angiogenesis upon activation by growth factor or integrin receptors. PI3Ks are lipid kinases, which can be divided into three classes: Class I, II, and III. Class I PI3Ks are activated by growth factor receptors or G-protein coupled receptors that are subdivided into Class IA and Class IB enzymes, respectively.<sup>1</sup> Class IA PI3Ks exist as heterodimers that contain one of three PI3K catalytic subunits (PI3K $\alpha$ , PI3K $\beta$ , and PI3K $\delta$ ) and a p85 regulatory subunits, whereas Class IB PI3Ks consist of a PI3K $\gamma$  catalytic subunit and a p101 regulatory subunit.<sup>1</sup> Class I PI3Ks convert the membrane bound substrate PIP2 (4,5-phosphatidylinositolbisphosphate) to PIP3 (3,4,5-phosphatidylinositoltrisphosphate), which provides lipid docking sites for the pleckstrin homology domains of the effector kinases PDK1 and Akt.<sup>1</sup> PTEN and other phosphatases negatively regulate PI3K by dephosphorylation of PIP3 to PIP2, attenuating further downstream signaling.<sup>1</sup> Class II PI3Ks display the ability to phosphorylate phosphatidylinositol and phosphatidylinositol

4-phosphate and are generally resistant to class I inhibitors. Class III PI3Ks phosphorylate only phosphatidylinositol to generate phosphatidylinositol 3-phosphate. The sole member of this class, known as Vps34, functions in protein trafficking and autophagy.<sup>2</sup> A fourth class of PI3K-related enzymes (PIKK), which contains a catalytic core similar to the PI3Ks, is involved in tumor growth and DNA-damage response as mediated by mTOR and DNA-dependent protein kinase, respectively.<sup>3</sup>

Upon formation of PIP3 by class I PI3Ks, PDK1 is recruited to the plasma membrane and in turn phosphorylates Akt, a serine/threonine kinase that integrates multiple signaling pathways involved in growth and metabolism regulation.<sup>4</sup> The activation of Akt results in phosphorylation of several proximal substrates, including mTOR and PRAS40, which triggers a cascade of signaling events that culminates in the activation of mTOR, a serine/threonine kinase that regulates cellular growth, nutrient metabolism, and protein translation. Class IA PI3Ks, and PI3K $\alpha$  in particular, are promising therapeutic targets for cancer based on the identification of activating mutations in the PI3K $\alpha$  catalytic subunit and loss of function of its negative regulator PTEN in a notable percentage of solid human tumors representing, breast, prostate, ovarian, colorectal cancer, and glioblastoma.<sup>5</sup> In addition, PI3Ks are activated upstream by known oncogenes such as HER2, EGFR, and Ras, all of which lead to aberrant activation of the pathway. Accordingly, pharmaceutical and academic laboratories are actively pursuing inhibitors of the central nodes of the PI3K/Akt/mTOR pathway, and PI3K $\alpha$  inhibitors in particular, for the treatment of human cancers.<sup>6</sup> Deregulation of the mTOR pathway has also been strongly

\*To whom correspondence should be addressed. E-mail: sutherland.dan@gene.com; phone: 650-225-2061; fax: 650-225-3171.

<sup>a</sup> Abbreviations: Akt, protein kinase B; DMF, dimethylformamide; DMSO, dimethylsulfoxide; EGFR, epidermal growth factor receptor 1; HER2, epidermal growth factor receptor 2; PEG, polyethylene glycol; PRAS40, proline-rich Akt substrate of 40 kDa; PI3K, phosphoinositide 3-kinase; PDK1, pyruvate dehydrogenase kinase isoform 1; PTEN, phosphatase and tensin homologue; pS6 RP, phosphorylated S 6 ribosomal protein; mTOR, mammalian target of rapamycin; TFA, trifluoroacetic acid; THF, tetrahydrofuran; DCE, dichloroethane; SAR, structure activity relationships.

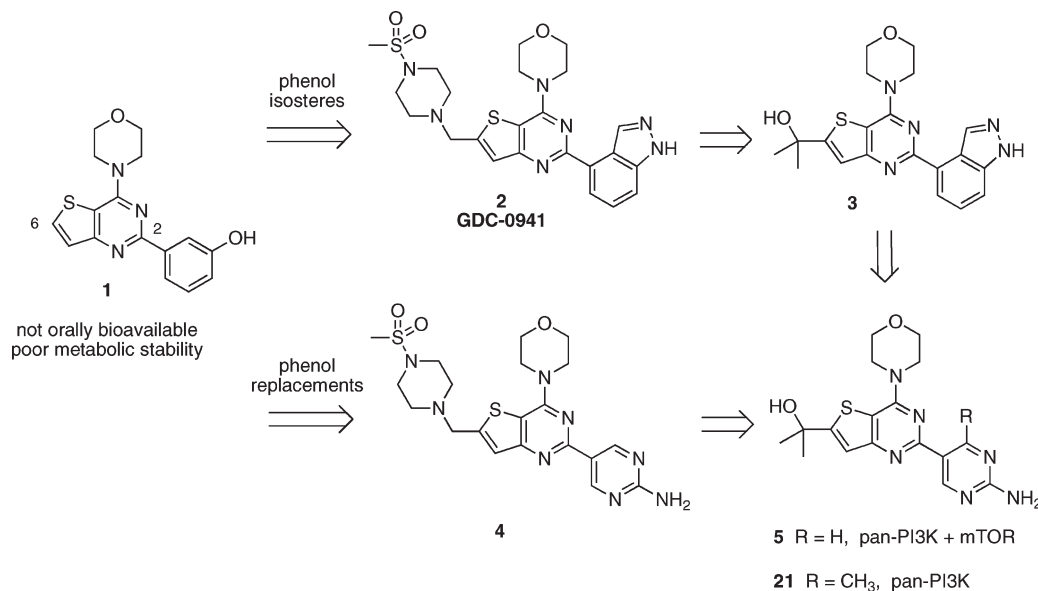


**Figure 1.** Discovery of compounds **5** and **21**, starting from phenols **1** and **2** (GDC-941).

implicated in cancer and inhibitors of this pathway are currently under clinical development.<sup>3b</sup> In addition, mTOR is a validated target in humans as demonstrated by the clinical use of Torisel (temsirolimus), approved for the treatment of advanced renal cell. Because both PI3K and mTOR are known to activate Akt independently, developing dual inhibitors of both PI3K $\alpha$  and mTOR is a potential strategy for generating more effective therapeutics for the treatment of human cancer.<sup>7</sup>

The discovery of the pan isoform ( $\alpha$ ,  $\beta$ ,  $\delta$ ,  $\gamma$ ) PI3K inhibitor, **2**, starting from the simple morpholino thienopyrimidine **1** has previously been described.<sup>8</sup> Key discoveries leading to the clinical compound **2** were the identification of an indazole as a phenolic isostere which significantly improved the oral bioavailability of the class and the addition of a piperazinomethane sulfonamide substituent to the C-6 position of the thienopyrimidine core that improved potency and metabolic stability relative to compound **1**.

Herein we describe our efforts to identify novel PI3K inhibitors that are structurally diverse from **2** and that have varying activity toward mTOR. In order to do this, we examined nonisostere replacements of the phenol resulting in new interactions within the same binding site, highlighted by the aminopyrimidine **4**, a compound that possessed increased mTOR potency relative to **2**. We also strove to remove potential sites of metabolism and reduce the molecular weight of the lead, resulting in tertiary alcohol **3**. These two directions of research were continued, culminating in the discovery of **5**, a low molecular weight, potent dual inhibitor of pan-PI3 kinases and mTOR. Following this, we discovered **21**, a structurally similar compound to **5**, which lacked mTOR but maintained pan-PI3K inhibitory activity.

### Synthesis

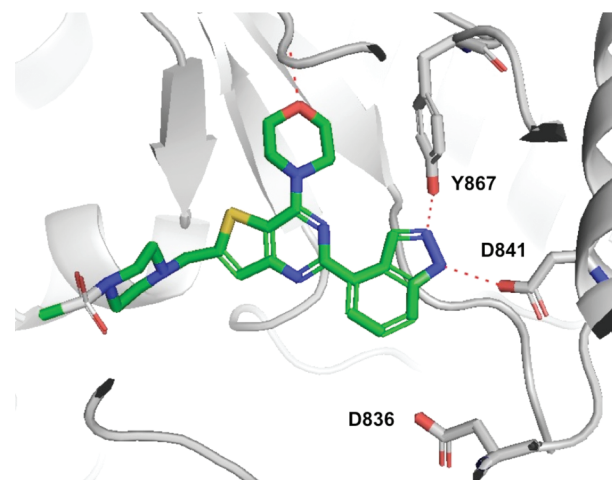
Compounds were prepared generally in a two-step process from common intermediate **6** (Scheme 1). In all cases, the C-6 position of the thienopyrimidine was functionalized prior to performing a Suzuki coupling with the C-2 aryl chloride and the corresponding boronic ester or acid to yield the 2-aryl thienopyrimidines. Compounds **4** and **10–16** were prepared

following similar procedures previously described in this journal, where DMF was used as an electrophile to prepare aldehyde **7** followed by reductive amination and Suzuki coupling.<sup>8</sup> Aldehyde **7** was also used to prepare compounds **17** and **18** by either reduction with sodium borohydride or addition of methyl Grignard to give the primary and secondary alcohols, respectively. The alcohol intermediate **9** could be converted to the acylated amine **19** through a series of steps that include bromination, transformation to an amine, acylation, and coupling. Alternatively, the anion of **6** could be trapped with acetone to give a tertiary alcohol which was subsequently used in a cross coupling reactions to generate compounds **3** and **5**.

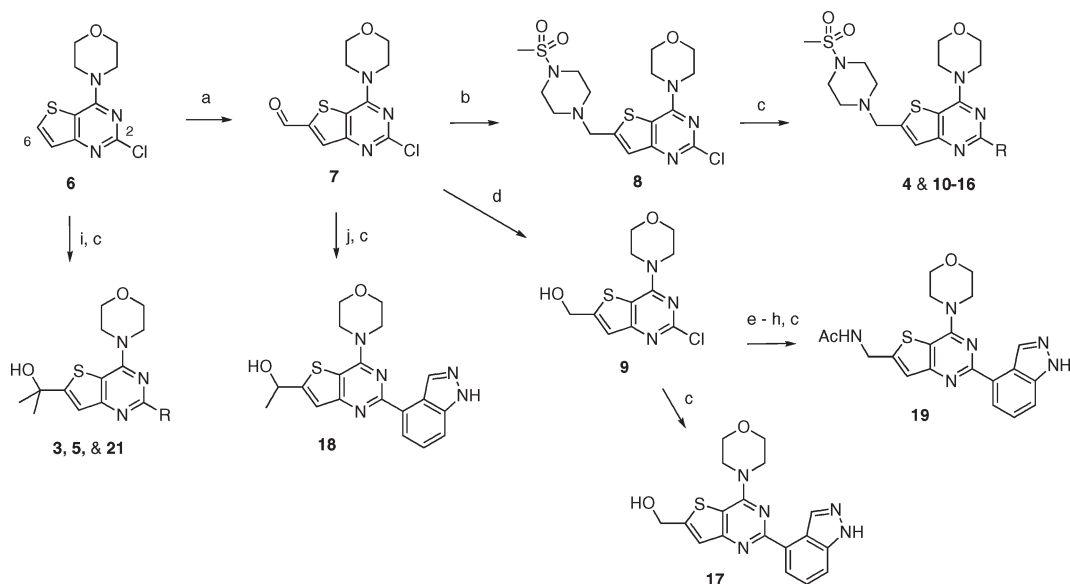
### Results and Discussion

The potency of each compound for inhibition of purified, recombinant PI3K isoforms  $\alpha$ ,  $\beta$ ,  $\gamma$ ,  $\delta$  was determined using a competitive displacement fluorescence polarization assay monitoring formation of the PIP3 product (Table 1).

Despite some minor differences in potency for the isoforms, the compounds in Table 1–3 were generally pan-inhibitors of



**Figure 2.** Crystal Structure of **2** in PI3K $\gamma$ .

**Scheme 1.** Synthesis of compounds found in Tables 1–3<sup>a</sup>

<sup>a</sup> Reagents and conditions: (a) *n*BuLi, THF,  $-78^{\circ}\text{C}$ , DMF; (b) *N*-sulphonylpiperazine, 1,2-DCE,  $\text{HC}(\text{OCH}_3)_3$ ,  $\text{Na}(\text{OAc})_3\text{BH}$ ; (c) boronic acid/ester,  $\text{Pd}(\text{PPh}_3)_2\text{Cl}_2$ ,  $\text{NaHCO}_3$ ,  $\text{H}_2\text{O}$ ,  $\text{CH}_3\text{CN}$ , microwave,  $150\text{--}140^{\circ}\text{C}$ , 15–30 min; (d)  $\text{NaBH}_4$ , MeOH; (e)  $\text{PBr}_3$ , benzene,  $80^{\circ}\text{C}$ , 1 h; (f) phthalimide,  $\text{K}_2\text{CO}_3$ , DMF, 20 h; (g)  $\text{N}_2\text{H}_4$ , MeOH,  $65^{\circ}\text{C}$ , 1 h; (h)  $\text{AcCl}$ ,  $\text{CH}_2\text{Cl}_2$ , rt, 16 h; (i) *n*BuLi, THF,  $-78^{\circ}\text{C}$ , acetone; (j)  $\text{MeMgBr}$ , THF,  $0^{\circ}\text{C}$ .

**Table 1.** Inhibition of PI3K $\alpha$ ,  $\beta$ ,  $\gamma$ ,  $\delta$ , and Cancer Cell Proliferation for Phenol Replacements for Compounds **2**, **4**, and **10–16**<sup>a</sup>

Compound	R1	IC <sub>50</sub> (nM)		IC <sub>50</sub> (μM)	
		PI3K $\alpha$	PI3K $\beta/\delta/\gamma$	PC3	MCF7.1
<b>2</b>		3.0	32/3.0/66	0.39	0.34
<b>10</b>		1.6	11/0.9/20	0.021	0.036
<b>11</b>		21	14/12/19	1.8	1.4
<b>12</b>		2900	5400/310/5100	ND	ND
<b>13</b>		430	ND	3.7	3.7
<b>14</b>		1.8	14/1.4/15	0.075	0.32
<b>15</b>		240	1400/100/1300	1.2	2.7
<b>16</b>		5.5	60/6.6/33	0.27	0.20
<b>4</b>		2.0	38/2.4/8.4	0.30	0.13

<sup>a</sup>ND = not determined.

the class I PI3-Kinases, with the greatest fold-selectivity for PI3K $\alpha$  of approximately 20-fold versus other PI3K isoforms. The antiproliferative activity was compared in the PTEN-null human tumor prostate cancer cell line PC3 and the PI3K $\alpha$  mutant breast cancer cell line MCF7.1. The clinical lead **2** has biochemical potencies of 3 nM, 32 nM, 3 nM, and 66 nM, versus PI3K  $\alpha$ ,  $\beta$ ,  $\delta$ , and  $\gamma$ , respectively, and cellular antiproliferative potencies in the PC3 and MCF7.1 cell lines of  $0.39\ \mu\text{M}$ , and  $0.34\ \mu\text{M}$ , respectively.

In order to design phenol replacements, we relied on X-ray crystal structures of **1** and **2** bound to PI3K $\gamma$  to observe the interactions that were contributing to the potency of these compounds as well as to evaluate the potential for other beneficial interactions. All four Class I PI3K isoforms are highly homologous within the active site and all residues discussed herein are conserved. As previously described, the morpholine in both molecules makes a key contact with the backbone NH of the hinge and is critical for potency.<sup>9</sup> The thienopyrimidine core can direct substituents toward solvent-exposed regions of the binding site from the C-6 position of the heterocycle as seen in **2**, and can position a C-2 aryl group into an affinity pocket, (exemplified by the indazole of **2**, Figure 2). From the X-ray cocrystal structure of PI3K $\gamma$  and **2** it was observed that the indazole 2-nitrogen makes a key hydrogen bond with the OH of Tyr 867 and the indazole NH forms an interaction with Asp 841. We recognized that there were a number of potential hydrogen bonding interactions that were not utilized by the indazole of **2** or the phenol of compound **1**. We theorized that these residues, Asp 836 as an example (PI3K $\gamma$  numbering), could form productive binding partners with a variety of structures that were neither phenols nor phenol isosteres.

Synthetically, the C-2 aryl group was installed at the last step of the synthesis and could easily be modified with a large number of boronic acids or esters. As a comparison to **2**, compound **10** was very potent (Table 1), but as previously described,<sup>8</sup> lacked oral bioavailability. In contrast to **10**, the

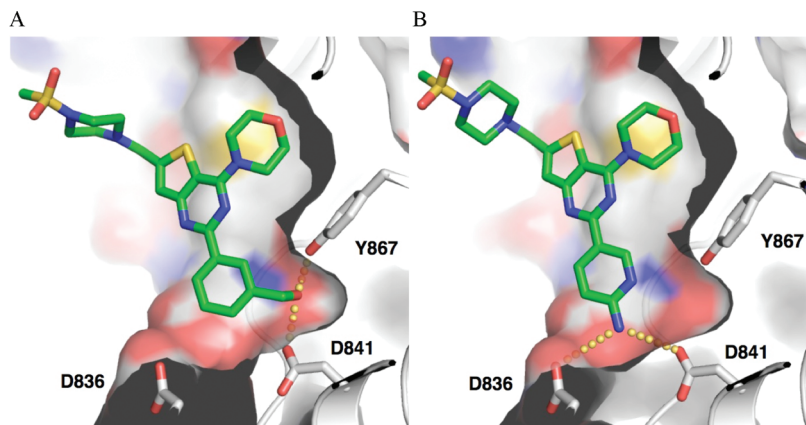


**Figure 3.** Crystal structures of **14** (panel A) and **16** (panel B) bound to PI3K $\gamma$ .

**Table 2.** Inhibition of PI3K $\alpha$  and PC3 Cancer Cell Proliferation; Hepatic Clearance Calculated from in Vitro Rat Liver Microsome Incubations; and Pharmacokinetic Results for Compounds Intravenously and Orally Dosed in Rats for Alcohol Analogues<sup>a</sup>

Compound	R1	R2	IC <sub>50</sub> ( $\mu$ M)		Clearance (rat, mL/min/kg)		F%
			PI3K $\alpha$	PC3	In Vitro	In Vivo	
<b>17</b>		4-indazole	0.029	1.2	170	ND	ND
<b>18</b>		4-indazole	0.028	1.1	95	101	17
<b>3</b>		4-indazole	0.022	1.4	40	16	29
<b>19</b>	AcHN-	4-indazole	0.016	1.5	40	86	34
<b>5</b>			0.0034	0.33	23	9	83

<sup>a</sup> Male Sprague–Dawley rats were dosed with mono TFA salts of each compound intravenously at 1 mg/kg and orally at 2 mg/kg as a solution in 5% DMSO/76% PEG400. Hepatic clearance was predicted from liver microsome incubations using the “in vitro  $t_{1/2}$  method”.<sup>11</sup>

**Table 3.** IV and PO PK Data for **5** in Mouse, Rat, Cynomolgus Monkey, and Dog<sup>a</sup>

species	in vitro Cl (mL/min/kg)	IV (1 mg/kg)			PO			
		in vitro Cl (mL/min/kg)	Vss (L/kg)	dose (mg/kg)	C <sub>max</sub> ( $\mu$ M)	AUC ( $\mu$ M*h)	F%	PPB%
mouse	45	17	2.8	5	2.1	14	100	64
rat	23	9	2.8	5	2.2	21	83	49
cyno	5.4	15	3.0	2	1.1	3.8	62	79
dog	1.8	1.6	1.6	2	4.4	63	100	73

<sup>a</sup> Female nu/nu mice were dosed orally with compounds as a solution in 60% PEG.

unsubstituted phenyl derivative **13** was over 400-fold less potent, highlighting the critical interaction that the phenol

has with Asp 841. Potency was regained by 3-hydroxymethyl phenyl **14** and demonstrated that activity could be attained

without directly mimicking the phenol. 3-Substituted pyridyl **11** was also capable of recovering activity whereas the 4-pyridyl **12** could not. On the basis of this SAR, it was thought that 3-pyridyl **11** could be making contacts to Tyr867 and Asp841 through a water-mediated H-bond. Interestingly, the crystal structure of **14** shows a clear interaction with the benzylic alcohol and Tyr 867 and Asp 841, anticipating the position of a potential water molecule bound to a pyridyl ring and this same tyrosine, strengthening this hypothesis (Figure 3A).

Aminopyridine **16** and aminopyrimidine **4** had excellent potencies, and analysis of crystal structures revealed potential H-bonding interactions with Asp 841 and Asp 836 (H-bonding distances are 3.2 and 3.6 Å, respectively for **16**, Figure 3B). These two compounds maintain the heterocyclic ring nitrogen/s similar to 3-pyridyl **11** while also increasing the acidity of the hydrogen on the para amino group relative to aniline **15**, a molecule that was 100-fold less potent than aminopyrimidine **4** ( $pK_a$ 's for the  $-NH_2$  of aniline, 2-aminopyridine, and 2-aminopyrimidine are 30.6, 27.7, and 25.3, respectively).<sup>10</sup> The substitutions of the phenol with either the aminopyridine or aminopyrimidine, in **16** and **4**, also greatly improved the PK profile in rodents, leading to good exposure, in contrast to the primary alcohol **14** which had 0% oral bioavailability. As an example, when dosed as a solution at 5 mg/kg in the rat, aminopyrimidine **4** had a moderate clearance of 24 mL/min/kg, a volume of distribution of 5.6 L/kg, and 75% oral bioavailability. However, both **4** and **16** had moderate to high clearance in male beagle dogs (22 and 16 mL/min/kg, respectively) that were not predicted by in vitro microsomal stability data (predicted hepatic clearance of 4.8 and 0.5, respectively) nor could they be explained via phase II metabolism. Thus, metabolic stability was an area for further optimization.

In parallel, we were also interested in modifying the physicochemical and pharmacodynamic (PD) properties of the molecule by modifying the 6 position of the thienopyrimidine, a region that was both exposed to solvent and had the greatest degree of flexibility in terms of SAR. Primary, secondary, and tertiary alcohols **17**, **18**, and **3** were targeted as substitutions

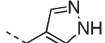
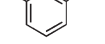
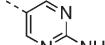
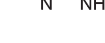
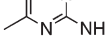
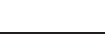
that were both small and would maintain some degree of solubility. Each had similar potencies in the biochemical assays but had in vitro and in vivo clearance that improved with increased steric bulk around the hydroxyl, presumably decreasing the likelihood of oxidation or conjugation of the alcohol (Table 2). Comparable potency and microsomal stabilities could also be obtained with the secondary amide **19**, but the clearance in the rat remained high in contrast to that of the tertiary alcohol, **3**.

The potency seen previously with the aminopyrimidine **4** along with the favorable pharmacokinetic properties of **3** prompted us to make **5**. This compound had improved potency and overall pharmacokinetic parameters relative to **3**. The increase in potency gained in going from an indazole to the aminopyrimidine was consistent with most compounds that had matched R1 substituents other than the optimized piperazine-sulfonamide found in **2**. The promising PK in rat translated well across species resulting in low to moderate clearances and good oral bioavailability in mice, dogs, and Cynomolgus monkeys (Table 3).

Male Sprague–Dawley rats were dosed orally with compounds as a solution in 5% DMSO/76% PEG400. Male Cynomolgus monkeys and male beagle dogs were dosed orally with the HCl salt of the compounds as a suspension in 0.5% methylcellulose/0.2% Tween-80.

**mTOR Activity.** In addition to potency against PI3K, we discovered that several compounds had increased potency for mTOR relative to **2** (Table 4). For the indazoles, **2** and **3**, reduction in the size of the left-hand portion of the molecule from the sulfonyl piperazine to the tertiary alcohol increased mTOR potency slightly while reducing PI3K $\alpha$  potency. On the other hand, **4** and **5** showed similar and increased mTOR inhibition regardless of the left-hand side group, suggesting that for these compounds the aminopyrimidine is driving most of the potency for both PI3K and mTOR inhibition. Further evaluation of the R2 position led to the 6-methyl substituted **20** and **21** which had >200 fold selectivity for mTOR while maintaining identical potency for PI3K $\alpha$  relative to their unsubstituted precursors. Overall, potency in the PC3 cell line appeared to correlate well with the PI3K $\alpha$

**Table 4.** Inhibition of PI3K Isoforms, mTOR, and Cancer Cell Proliferation for Selected Compounds

Compound	R1	R2	IC <sub>50</sub> (nM)			IC <sub>50</sub> (μM)	
			PI3K $\alpha$	mTOR	PI3K $\beta/\delta/\gamma$	PC3	MCF7.1
<b>2</b>	A		3.0	310	32/3.0/66	0.28	0.33
<b>3</b>	B		22	130	ND	1.3	1.4
<b>4</b>	A		1.9	29	38/2.4/8.4	0.31	0.13
<b>5</b>	B		3.4	30	12/16/16	0.33	0.18
<b>20</b>	A		1.1	880	6.2/0.7/5.2	0.23	0.29
<b>21</b>	B		3.5	750	25/5.2/15	0.49	0.28

biochemical potency and was not dramatically influenced by mTOR potency.

To better understand the potency and selectivity of our compounds, we examined the residue differences between mTOR and PI3K isoforms in the vicinity of the inhibitors. All of the PI3K $\gamma$  residues discussed throughout are identical to those found in PI3K $\alpha$ . Our analysis suggests that mTOR has identical residues corresponding to Tyr867 and Asp841 and a homologous Glu in the place of Asp836 (Figure 4). The binding site of the two enzymes also differ in the upper portion of the ATP binding pocket where Met804 and Ile831 of PI3K $\gamma$  align to Ile2163 and Leu2186 in mTOR, respectively, potentially altering the hydrophobic surface in this region.

The increased potency for mTOR in compounds with an aminopyrimidine relative to those with an indazole is possibly because this portion of the molecule is adjacent to Asp836(PI3K $\gamma$ )/Glu2190(mTOR). This residue resides on a loop which is one amino acid longer in mTOR than in PI3K $\gamma$ . mTOR's Glu2190 likely adopts different conformations and experiences different flexibility compared to PI3K $\gamma$ 's Asp836, such that its favorable interactions with the aminopyrimidine are disrupted by the indazole, giving rise to the observed SAR.

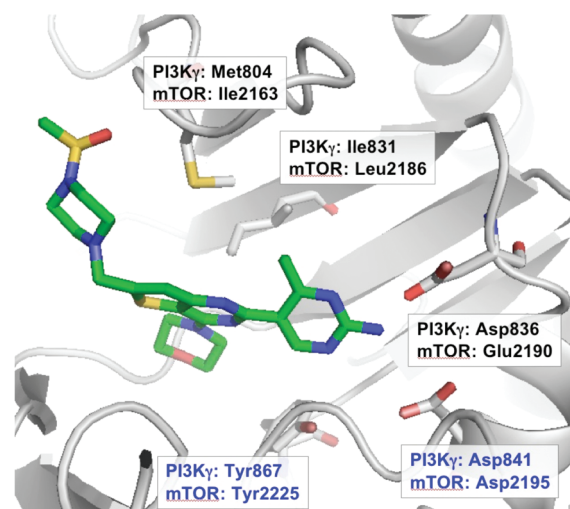


**Figure 4.** Structure of **20** bound to PI3K $\gamma$ . Residues labeled in blue are identical in mTOR, while residues in black align to different amino acids in mTOR.

**Table 5.** Potency and Mouse PK Data for **5** and **21**<sup>a</sup>

compd	IC <sub>50</sub> (nM)					mouse PK (1 mg/kg iv/5 mg/kg po)					
	PI3K $\alpha$	PI3K $\beta/\delta/\gamma$	mTOR	PC3	MCF7.1	Cl (mL/min/kg)	V <sub>ss</sub> (L/kg)	AUC ( $\mu$ M*h, po)	T <sub>1/2</sub> (h, po)	F%	PPB% mouse
<b>5</b>	3.4	12/16/16	32	330	180	17	2.8	13.7	3.6	100	64
<b>21</b>	3.5	25/5.2/15	740	490	280	51	3.0	4.8	4.6	100	73

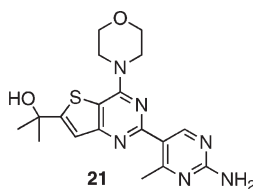
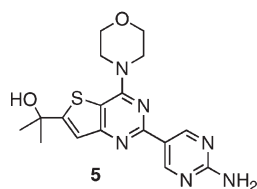
<sup>a</sup> Female nu/nu mice were dosed orally with the HCl salt of each compound as a solution intravenously in 5% DMSO/5% cremophor. Compound **5** was dosed orally as a solution in 60% PEG and **21** was dosed orally in 0.5% methylcellulose/0.2% Tween-80. AUCs for **5** when dosed in MCT were equivalent to the AUC reported in PEG.

To rationalize the dramatic shifts in selectivity derived from the addition of a single methyl group onto the aminopyrimidine, we examined a crystal structure of **20** with PI3K $\gamma$  (Figure 4). The 4-methyl group, as expected, twists the amino pyrimidine ring out of the plane of the thienopyrimidine in contrast to the unsubstituted aminopyrimidine analogues (not shown). Furthermore, steric clashes with Tyr867 cause the 4-methyl to point away from that residue and toward the upper surface of the ATP binding pocket where differences in mTOR and PI3K exist, presumably resulting in the observed selectivity.

**Kinase Selectivity.** Compound **2**, the pan-PI3K inhibitor currently in clinical oncology trials, displays an excellent selectivity profile relative to other Ser/Thr and Tyr kinases.<sup>8</sup> The highly optimized **5** and **21**, which each display approximately equipotent inhibition of Class I PI3K isoforms, were submitted for screening in a 142 kinase panel provided by Invitrogen's SelectScreen service. Of these kinases, only three were subject to greater than 50% inhibition by **5**, and none were inhibited greater than 80% when tested at 1  $\mu$ M. Subsequently measured IC<sub>50</sub>s demonstrated that **5** is more than 100-fold selective for PI3K $\alpha$  over these three unrelated kinases (Aurora A IC<sub>50</sub> > 10  $\mu$ M, MLK1 IC<sub>50</sub> = 591 nM and SYK IC<sub>50</sub> = 371 nM). In the same panel, all kinases displayed less than 50% inhibition at 1  $\mu$ M (or IC<sub>50</sub>'s > 1  $\mu$ M) by **21**. Several members of the related PIK family kinases were also screened at Invitrogen: **5** displayed relatively weak inhibition of PIK3 C2 alpha and PIK3 C2 beta (65 and 78% inhibition at 1  $\mu$ M, respectively), but no significant inhibition of hVPS34 or PI4K beta was seen. Similarly, **21** caused no significant inhibition of PIK3 C2 alpha, hVPS34, or PI4K beta, and 81% inhibition of PIK3 C2 beta at 1  $\mu$ M (data not shown). Thus, both of these molecules were deemed sufficiently selective for PI3K $\alpha$  or PI3K $\alpha$  and mTOR to warrant further evaluation in human tumor xenograft efficacy studies.

#### Pharmacokinetic Data

Two representative compounds, **5** and **21**, were chosen as examples of a dual pan-PI3K + mTOR inhibitor and a pan-PI3K inhibitor (Table 5). Each of these compounds displayed promising PK parameters in mice, suggesting that both molecules could achieve sufficient exposure to warrant testing their antitumor efficacy in human tumor xenograft models. Compound **5** achieved an almost 2.5-fold greater exposure in vivo



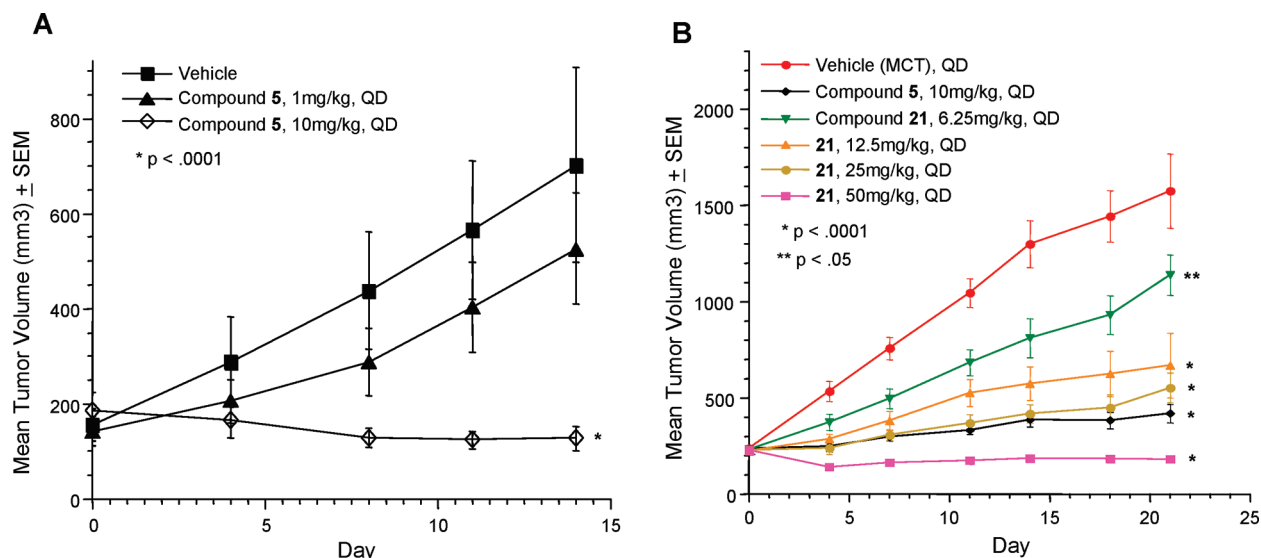


**Figure 5.** In vivo efficacy of **5** versus PC3 prostate cancer xenografts and compounds **5** and **21**, versus MCF7.1 breast cancer xenografts. (A) Nu/nu (nude) female mice bearing PC3 tumors established from human prostate cancer cells implanted subcutaneously were dosed orally either with **5** at the indicated concentrations as a solution/suspension in vehicle (0.5% methylcellulose/0.2% Tween-80) or with vehicle daily (QD) for 14 days. (B) Nu/nu (nude) female mice bearing tumors established from MCF7.1 breast cancer cells implanted subcutaneously were dosed orally with vehicle, or as a solution/suspension of **5** or **21** at the indicated concentrations in the aforementioned vehicle daily (QD) for 21 days. Dunnett *t* test was used to calculate *p*-values comparing the drug-treated groups with vehicle control group at the end of dosing either on day 14 or 21.

than **21** when dosed at 5 mg/kg, exposure differences which seemed to be maintained at higher doses. Additionally, **21** showed 2 and 0.5 times less potency on PC3 and MCF7.1 cells lines, respectively, than **5**. These important differences in cellular potency and in vivo exposure were taken into consideration as we designed and interpreted results from in vivo efficacy studies.

**Anti-Tumor In Vivo Efficacy.** The favorable in vitro potency and PK profiles of **5** and **21** (Table 5) prompted us to test these compounds in vivo against the same human cancer cell lines used in the in vitro cellular assays, but grown as subcutaneous xenografts in nude mice. For PC3, a human prostate cancer cell line that is PTEN  $-/-$ , once daily oral dosing with 10 mg/kg of **5** for 14 continuous days resulted significant in tumor regressions, with 6 partial regressions (50–99% tumor inhibition) and 1 complete regression (100% tumor inhibition) out of 10 animals (Figure 5A). The mean reduction in tumor volume at day 14 compared to vehicle-treated animals was 89%. At a 10-fold lower dose of 1 mg/kg, **5** showed no statistically significant efficacy in the PC3 prostate cancer xenograft model. All doses tested were tolerated and did not cause significant body weight loss (data not shown).

To confirm and compare in vivo efficacy, **5** and **21** were examined in the human MCF7.1 breast cancer xenograft model that harbors a PI3K $\alpha$  activating mutation. Mice bearing xenografts were dosed orally once daily with 10 mg/kg of **5** or escalating doses of **21** from 6.25 mg/kg to 50 mg/kg for 21 continuous days. Similar to observations made in the PC3 prostate cancer xenograft model, 10 mg/kg of **5** resulted in 73% tumor growth inhibition at day 21 when compared to vehicle control animals (Figure 5B). Compound **21** also displayed 88% tumor growth inhibition at 50 mg/kg and doses as low as 6.25 mg/kg were also efficacious (28% tumor growth inhibition;  $p < 0.05$ ) (Figure 5B). Comparable efficacy was observed with 10 mg/kg of **5** and 25 mg/kg of **21** and was attributed to both compounds

showing similar drug exposures at these doses (data not shown). All doses of **21** and **5** tested were tolerated with insignificant body weight loss observed (data not shown).

The similar efficacy profiles of **21** and **5** suggested that the effect on PI3K/Akt pathway markers might be similar in vivo. Upon completion of continuous dosing (up to day 21), MCF7.1 tumors were collected and analyzed to assess the PD regulation of the primary PI3K/Akt/mTOR pathway markers, phospho-Akt (pAkt), phospho-PRAS40 (pPRAS40) and phospho-S6RP, (pS6RP), relative to total protein marker levels, respectively. Doses as low as 6.25 mg/kg of **21** caused significant suppression of all three pathway markers within 1 h of treatment (Figure 6A–C) and was comparable to 10 mg/kg of **5**. However, at 4 h, maximum suppression of all three markers was observed only at 25 mg/kg of **21** and at 10 mg/kg of **5**. These same doses showed equivalent antitumor responses for both compounds versus the MCF7.1 xenograft, suggesting that in this model the PI3K/Akt pathway must be suppressed for at least 4 h in order to achieve maximum efficacy. Furthermore, as observed in the efficacy study, the PD response to **21** and **5** correlated well with plasma drug levels (data not shown). Thus, when achieving comparable levels of drug exposure, **5** and **21** showed a similar suppression of the PI3K pathway and consequently, a similar efficacy profile against MCF7.1 breast tumors.

## Conclusion

Two potent, selective, and efficacious pan-PI3K inhibitors have been discovered. Using **1** as a template, SAR was developed that led to the replacement of a phenol with an aminopyrimidine resulted in improved exposure in rodents. Additionally, the piperazine-sulfonamide of **4** was replaced with a tertiary alcohol to give **5**, reducing the molecular weight and increasing the metabolic stability relative to **4**. Compound **5** has excellent pharmacokinetic properties in all species tested

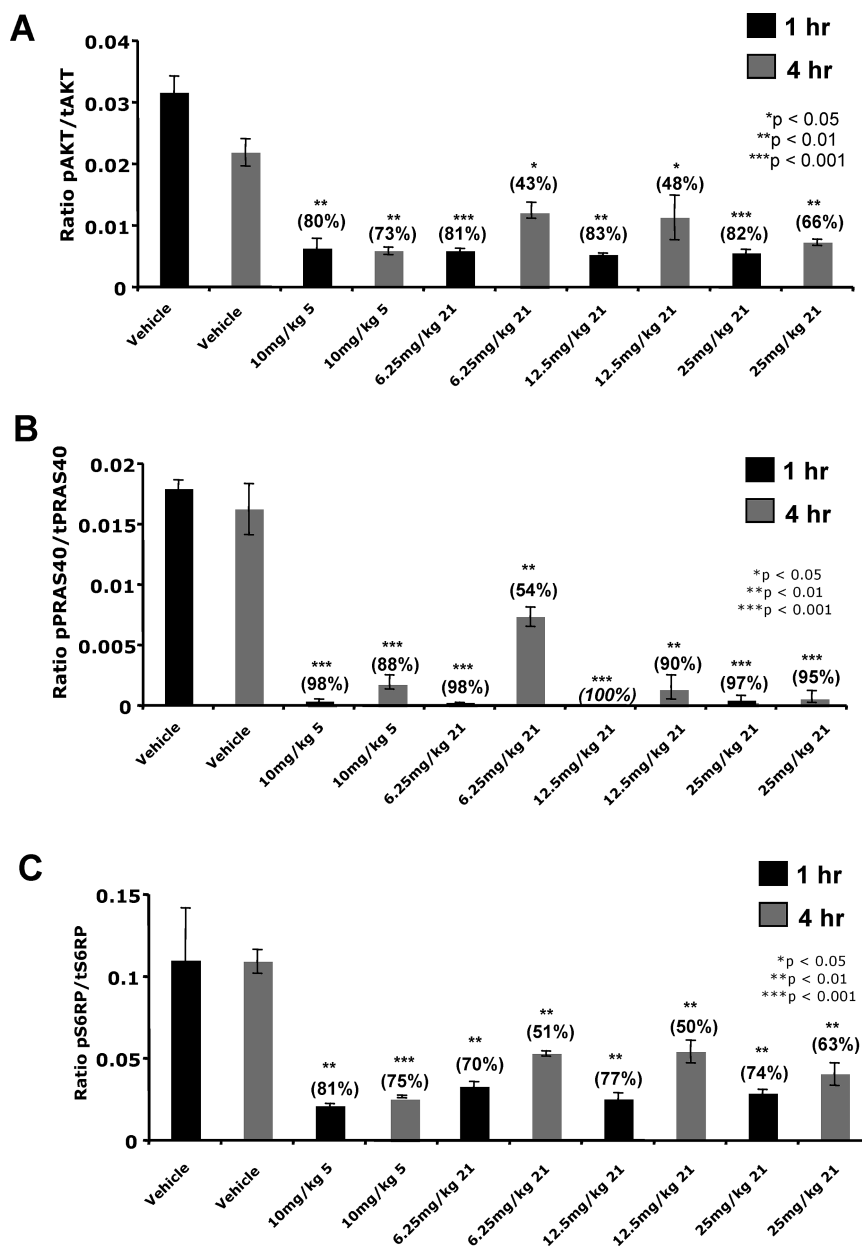


**Figure 6.** Effect of **5** and **21** on PD markers in the MCF7.1 breast cancer xenograft model after 21 days of continuous dosing. Tumors were excised from animals 1 and 4 h after the last administered dose on day 21 and processed for analysis of PI3K/Akt pathway markers as described in Methods. (A) Levels of pAkt (Ser<sup>473</sup>) and total Akt were measured by electrochemiluminescence using Meso Scale Discovery according to manufacturer's instructions (Gaithersburg, MD). (B) Levels of pPras40 (Thr<sup>246</sup>) and total Pras40 were measured by ELISA at an absorbance of 450 nm as described in Methods. (C) pS6RP (Ser<sup>235/236</sup>) and total S6RP were assessed using assays measuring electrochemiluminescence from Meso Scale Discovery (Gaithersburg, MD) according to manufacturer's instructions. (%) = % of phospho-protein suppression compared to vehicle control groups (100%); *p*-values determined by Student's *t* test.

and is remarkably selective against >130 kinases. Evaluation of structure–activity relationships around this series revealed a method for modulating potency against mTOR, offering a significant opportunity to expand upon the therapeutic potential of this chemical series. Specifically, the addition of a 4-methyl group on the pyrimidine modulated the mTOR potency, resulting in **21**. Compound **5** was profiled in tumor models in which the PI3K pathway is activated such as PC3 prostate cancer and MCF7.1 breast cancer xenograft models and was highly efficacious *in vivo* at 10 mg/kg when administered orally on a daily schedule. The mTOR selective **21** was also profiled in the MCF7.1 tumor model and was found to have equivalent efficacy and PD responses to the dual

PI3K/mTOR inhibitor **5** when differences in exposure were taken into account. The fact that MCF7.1 cells possess an activating mutation of PI3K $\alpha$  and are likely more dependent on this pathway may be one explanation for the apparent equivalency for these two compounds in this particular xenograft model, regardless of differences in mTOR potency. Both **21** (GNE-490) and **5** (GNE-493) are excellent tools to further evaluate the therapeutic potential of PI3K and dual PI3K/mTOR inhibitors in the treatment of cancer.

#### Experimental Procedures

**Chemistry.** All solvents and reagents were used as obtained. <sup>1</sup>H NMR spectra were recorded with a Bruker Avance DPX400



Spectrometer or a Varian Inova 400 NMR spectrometer, and referenced to tetramethyl silane. chemical shifts are expressed as  $\delta$  units using tetramethylsilane as the external standard (in NMR description, s, singlet; d, doublet; t, triplet; q, quartet; m, multiplet; and br, broad peak). Mass spectra were measured with a Finnigan SSQ710C spectrometer using an ESI source coupled to a Waters 600MS HPLC system operating in reverse mode with an X-bridge Phenyl column of dimensions 150 mm by 4.6 mm, with 5  $\mu$ m sized particles.

Compounds **2**, **6**–**8**, and intermediates in route to compounds **10**–**16** have been previously described in this journal.<sup>7</sup>

**2-(2-Chloro-4-morpholinothieno[3,2-*d*]pyrimidin-6-yl)propan-2-ol**. 4-(2-Chlorothieno[3,2-*d*]pyrimidin-4-yl)morpholine (20.0 g, mmol) was combined with THF (300 mL) and cooled to  $-78$  °C prior to slow addition of 2.5 M *n*-BuLi in hexane (40.6 mL) via an addition funnel to maintain a temperature below  $-70$  °C. The reaction was brought to  $-60$  °C and allowed to stir for 1 h. The reaction mixture was recooled to  $-78$  °C and acetone was added slowly via an addition funnel to maintain the temperature below  $-70$  °C. After stirring for 2 h, the reaction was quenched into a mixture of 1 N HCl (100 mL), water (600 g), and ice (600 g). The slurry was filtered and washed with water (150 mL) and dried in a vacuum oven overnight at 50 °C to yield 22.3 g of 2-(2-chloro-4-morpholinothieno[3,2-*d*]pyrimidin-6-yl)propan-2-ol (83.5% yield).

**2-(2-(2-Aminopyrimidin-5-yl)-4-morpholinothieno[3,2-*d*]pyrimidin-6-yl)propan-2-ol (5)**. 2-(2-Chloro-4-morpholinothieno[3,2-*d*]pyrimidin-6-yl)propan-2-ol (26.0 g), 5-(4,4,5,5-tetramethyl-1,3,2-dioxaborolan-2-yl)pyrimidin-2-amine (23 g), Na<sub>2</sub>CO<sub>3</sub> (17.6 g), dioxane (390 mL), and water (156 mL) were combined to give a light yellow suspension. The reaction mixture was degassed through several vacuum and purge cycles with N<sub>2</sub>. PdCl<sub>2</sub>(PPh<sub>3</sub>)<sub>2</sub> (1.116 g) was added followed by additional vacuum and purge cycles with N<sub>2</sub>. The reaction was then heated for 12 h at an internal temperature of 90 °C and then cooled to room temperature. Water (400 mL) was added and the mixture was allowed to stir for 1 h prior to filtration and an additional water wash (100 mL). The resultant gray solid was combined with THF (1 L), water (100 mL), and finally Florisil (52 g, 60–100 mesh) and stirred for 15 min prior to filtration. The Florisil was washed with two portions of THF (300 and 200 mL) and the filtrate was evaporated, suspended in EtOAc, heated to 80 °C for 1 h, and cooled to room temp. The resultant solid was filtered to give 25.8 g of **5** (85.5% yield). <sup>1</sup>H NMR (400 MHz, DMSO)  $\delta$  9.28 (s, 2H), 7.78 (bs, 1H), 7.52 (s, 1H), 4.11 (m, 4H), 3.80 (m, 4H), 1.60 (s, 6H). MS (ESI): *m/z* (M + H)<sup>+</sup> 373. Analytical LC-MS on an Agilent (1100/MSD) using a 3 mm  $\times$  100 mm SD-C18 analytical column and H<sub>2</sub>O/MeCN modified with 0.05% trifluoroacetic acid running a linear gradient from 5% MeCN to 95% MeCN monitored by UV wavelength 254 nm and ESI+ TIC MS showed 99% purity.

**2-(2-(2-Aminopyrimidin-5-yl)-4-morpholinothieno[3,2-*d*]pyrimidin-6-yl)propan-2-ol hydrochloride (5)**. 2-(2-(2-Aminopyrimidin-5-yl)-4-morpholinothieno[3,2-*d*]pyrimidin-6-yl)propan-2-ol (15.8 g) was suspended in 160 mL of methanol and combined with a solution of HCl in ethanol (1.25 M, 36 mL), stirred for 2 h, cooled to 0 °C, and filtered to give 14.8 g of the HCl salt of **5** (85.5% yield). <sup>1</sup>H NMR (400 MHz, DMSO)  $\delta$  9.28 (s, 2H), 7.78 (bs, 1H), 7.52 (s, 1H), 4.11 (m, 4H), 3.80 (m, 4H), 1.60 (s, 6H). MS (ESI): *m/z* (M + H)<sup>+</sup> 373. Analytical LC-MS on an Agilent (1100/MSD) using a 3 mm  $\times$  100 mm SD-C18 analytical column and H<sub>2</sub>O/MeCN modified with 0.05% trifluoroacetic acid running a linear gradient from 5% MeCN to 95% MeCN monitored by UV wavelength 254 nm and ESI+ TIC MS showed 99% purity. Anal. (C<sub>17</sub>H<sub>21</sub>ClN<sub>6</sub>O<sub>2</sub>S) C, H, N, Cl.

**3-[6-(4-Methanesulfonyl-piperazin-1-ylmethyl)-4-morpholin-4-yl-thieno[3,2-*d*]pyrimidin-2-yl]-phenol (10)**. A mixture of 4-morpholin-4-yl-2-[3-(1,1,2,2-tetramethyl-propylsilyloxy)-phenyl]-thieno[3,2-*d*]pyrimidine-6-carbaldehyde<sup>8</sup> (0.101 g, 0.221 mmol), 1-methanesulfonyl-piperazine hydrochloride (0.06 g, 1.3 equiv), acetic acid (13  $\mu$ L, 1.0 equiv), and triethylamine (42  $\mu$ L) was stirred in 1,2-dichloroethane (6 mL) at room temperature. To this was

added sodium triacetoxyborohydride (0.074 g, 1.6 equiv), and the reaction mixture was stirred for 1 day. The reaction mixture was then quenched with aqueous sodium bicarbonate solution, extracted exhaustively with chloroform, dried (MgSO<sub>4</sub>), and the solvent was removed in vacuo to yield an oil. This was purified using flash chromatography (silica, ethyl acetate/hexane to ethyl acetate to yield 2-[3-(*tert*-butyl-dimethyl-silyloxy)-phenyl]-6-(4-methanesulfonyl-piperazin-1-ylmethyl)-4-morpholin-4-yl-thieno[3,2-*d*]pyrimidine. To a solution of 2-[3-(*tert*-butyl-dimethyl-silyloxy)-phenyl]-6-(4-methanesulfonyl-piperazin-1-ylmethyl)-4-morpholin-4-yl-thieno[3,2-*d*]pyrimidine in THF (10 mL) cooled to 0 °C was added a 1.0 M solution of tetrabutyl ammonium fluoride in THF (84  $\mu$ L). After 30 min, the solvent was removed in vacuo and the residue was purified using flash chromatography (silica, 2% methanol in dichloromethane) and then triturated using dichloromethane/hexane to yield the title compound as a white solid (21 mg, 21%). <sup>1</sup>H NMR (400 MHz, CDCl<sub>3</sub>)  $\delta$  2.59 (m, 4H), 2.72 (s, 3H), 3.20 (m, 4H), 3.80 (m, 6H), 3.94–3.97 (m, 4H), 6.87 (d, *J* = 7.8 Hz 1H), 7.19–7.27 (m, 2H), 7.88 (m, 2H). MS (ESI): *m/z* (M + H)<sup>+</sup> 490. Analytical LC-MS using Waters XBridge Phenyl analytical column and H<sub>2</sub>O/MeCN modified with 0.1% formic acid running a linear gradient from 10% MeCN to 100% MeCN monitored by UV wavelength 210 nm and ESI+ TIC MS showed 100% purity.

**6-(4-Methanesulfonyl-piperazin-1-ylmethyl)-4-morpholin-4-yl-2-pyridin-3-yl-thieno[3,2-*d*]pyrimidine (11)**. A mixture of 2-chloro-6-(4-methanesulfonyl-piperazin-1-ylmethyl)-4-morpholin-4-yl-thieno[3,2-*d*]pyrimidine<sup>8</sup> (100 mg, 0.23 mmol), pyridine-3-boronic acid (57 mg, 2 equiv), sodium carbonate (95 mg, 3 equiv), water (1 mL), acetonitrile (3 mL), and PdCl<sub>2</sub>(PPh<sub>3</sub>)<sub>2</sub> (0.1 equiv) was heated to 140 °C for 30 min in the microwave. The reaction mixture was cooled, diluted with dichloromethane, washed with brine, dried (MgSO<sub>4</sub>), and the solvent was removed in vacuo. The residue was purified using flash chromatography (3% methanol in ethyl acetate) and then trituration with ether yielded the desired title compound as a white solid (84 mg, 77%). <sup>1</sup>H NMR (400 MHz, CDCl<sub>3</sub>)  $\delta$  2.68–2.72 (m, 4H), 2.82 (s, 3H), 3.29–3.33 (m, 4H), 3.90 (s, 2H), 3.90–3.94 (m, 4H), 4.05–4.10 (m, 4H), 7.33 (s, 1H), 7.34–7.38 (m, 1H), 8.68 (d, *J* = 5.6 Hz, 1H), 9.64 (s, 1H). MS (ESI): *m/z* (M + H)<sup>+</sup> 475. Analytical LC-MS using Waters XBridge Phenyl analytical column and H<sub>2</sub>O/MeCN modified with 0.1% formic acid running a linear gradient from 10% MeCN to 100% MeCN monitored by UV wavelength 210 nm and ESI+ TIC MS showed 100% purity.

**6-(4-Methanesulfonyl-piperazin-1-ylmethyl)-4-morpholin-4-yl-2-pyridin-4-yl-thieno[3,2-*d*]pyrimidine (12)**. Compound **12** was prepared from 2-chloro-6-(4-methanesulfonyl-piperazin-1-ylmethyl)-4-morpholin-4-yl-thieno[3,2-*d*]pyrimidine<sup>8</sup> according to a similar Suzuki coupling procedure as described for compound **11**, using 4-pyridyl boronic acid. Yield = 71%. <sup>1</sup>H NMR (400 MHz, CDCl<sub>3</sub>)  $\delta$  2.68–2.70 (m, 4H), 2.81 (s, 3H), 3.29–3.32 (m, 4H), 3.89–3.91 (m, 6H), 4.06–4.08 (m, 4H), 7.35 (s, H), 8.26 (dd, *J* = 4.5, 3.0 Hz, 2H), 8.72 (dd, *J* = 4.66, 3 Hz, 2H). MS (ESI): *m/z* (M + H)<sup>+</sup> 475. Analytical LC-MS using Waters XBridge Phenyl analytical column and H<sub>2</sub>O/MeCN modified with 0.1% formic acid running a linear gradient from 10% MeCN to 100% MeCN monitored by UV wavelength 210 nm and ESI+ TIC MS showed 100% purity.

**(4-(6-((4-(Methylsulfonyl)piperazin-1-yl)methyl)-2-phenylthieno[3,2-*d*]pyrimidin-4-yl)morpholine (13)**. Compound **13** was prepared from 2-chloro-6-(4-methanesulfonyl-piperazin-1-ylmethyl)-4-morpholin-4-yl-thieno[3,2-*d*]pyrimidine<sup>8</sup> according to a similar Suzuki coupling procedure as described for compound **11**, using phenyl boronic acid and purified on reversed phase HPLC. Yield = 59%. <sup>1</sup>H NMR (400 MHz, CDCl<sub>3</sub>)  $\delta$  8.33 (d, *J* = 7.2 Hz, 2H), 7.98 (s, 1H), 7.64 (t, *J* = 7.3 Hz, 1H), 7.57 (t, *J* = 7.4, 2H), 4.30–4.22 (m, 4H), 4.17 (s, 2H), 3.99–3.92 (m, 4H), 3.43 (br s, 4H), 2.96–2.89 (m, 4H), 2.85 (s, 3H). MS (ESI): *m/z* (M+H)<sup>+</sup> 474.2. Analytical LC-MS on an Agilent (1100/MSD) using a 3 mm  $\times$  100 mm SD-C18 analytical column and H<sub>2</sub>O/MeCN

modified with 0.05% trifluoroacetic acid running a linear gradient from 5% MeCN to 95% MeCN monitored by UV wavelength 254 nm and ESI+ TIC MS showed 97% purity.

**3-(6-((4-(Methylsulfonyl)piperazin-1-yl)methyl)-4-morpholinothieno[3,2-d]pyrimidin-2-yl)phenyl)methanol (14).** Compound 14 was prepared from 2-chloro-6-(4-methanesulfonyl-piperazin-1-ylmethyl)-4-morpholin-4-yl-thieno[3,2-d]pyrimidine<sup>8</sup> according to a similar Suzuki coupling procedure as described for compound 11, using 3-(hydroxymethyl)phenylboronic acid and purified on reversed phase HPLC. Yield = 62%. <sup>1</sup>H NMR (400 MHz, DMSO-*d*<sub>6</sub>) δ 8.35 (s, 1H), 8.26 (t, 1H), 7.59 (s, 1H), 7.47 (m, 1H), 4.61 (s, 2H), 4.04 (d, 2H), 3.83 (d, 2H), 3.31 (d, 2H), 2.96 (d, 2H), 2.96 ppm (s, 2H). MS (ESI): *m/z* (M + H)<sup>+</sup> 504.2. Analytical LC-MS on an Agilent (1100/MSD) using a 3 mm × 100 mm SD-C18 analytical column and H<sub>2</sub>O/MeCN modified with 0.05% trifluoroacetic acid running a linear gradient from 5% MeCN to 95% MeCN monitored by UV wavelength 254 nm and ESI+ TIC MS showed 98% purity.

**4-[6-(4-Methanesulfonyl-piperazin-1-ylmethyl)-4-morpholin-4-yl-thieno[3,2-d]pyrimidin-2-yl]-phenylamine (15).** Compound 15 was prepared from 2-chloro-6-(4-methanesulfonyl-piperazin-1-ylmethyl)-4-morpholin-4-yl-thieno[3,2-d]pyrimidine<sup>8</sup> according to a similar Suzuki coupling procedure for compound 11, using 4-(4,4,5,5-tetramethyl-1,3,2-dioxaborolan-2-yl)aniline. Yield = 83%. <sup>1</sup>H NMR (400 MHz, CDCl<sub>3</sub>) δ 2.67–2.71 (m, 4H), 2.81 (s, 3H), 3.29–3.33 (m, 4H), 3.89 (s, 2H), 3.89–3.93 (m, 4H), 4.08–4.12 (m, 4H), 6.75 (d, *J* = 8.6 Hz, 2H), 7.30 (s, 1H), 8.29 (d, *J* = 8.6 Hz, 2H). MS (ESI): *m/z* (M + H)<sup>+</sup> 489. Analytical LC-MS using Waters XBridge Phenyl analytical column and H<sub>2</sub>O/MeCN modified with 0.1% formic acid running a linear gradient from 10% MeCN to 100% MeCN monitored by UV wavelength 210 nm and ESI+ TIC MS showed 100% purity.

**5-[6-(4-Methanesulfonyl-piperazin-1-ylmethyl)-4-morpholin-4-yl-thieno[3,2-d]pyrimidin-2-yl]-pyridin-2-ylamine (16).** Compound 16 was prepared from 2-chloro-6-(4-methanesulfonyl-piperazin-1-ylmethyl)-4-morpholin-4-yl-thieno[3,2-d]pyrimidine<sup>8</sup> according to a similar Suzuki coupling procedure for compound 11, using 2-amino-5-(4,4,5,5-tetramethyl-1,3,2-dioxaborolan-2-yl)pyridine. Yield = 39%. <sup>1</sup>H NMR (400 MHz, CDCl<sub>3</sub>) δ 2.67–2.71 (m, 4H), 2.81 (s, 3H), 3.29–3.33 (m, 4H), 3.89 (s, 2H), 3.89–3.93 (m, 4H), 4.08–4.12 (m, 4H), 4.60–4.65 (br s, 2H), 6.57 (d, *J* = 8.6 Hz, 1H), 7.40 (s, 1H), 8.45 (dd, *J* = 8.6, 2.2 Hz, 1H), 9.17 (d, *J* = 2.2 Hz, 1H). MS (ESI): *m/z* (M + H)<sup>+</sup> 490. Analytical LC-MS using Waters XBridge Phenyl analytical column and H<sub>2</sub>O/MeCN modified with 0.1% formic acid running a linear gradient from 10% MeCN to 100% MeCN monitored by UV wavelength 210 nm and ESI+ TIC MS showed 99% purity.

**2-(2-(1H-indazol-4-yl)-4-morpholinothieno[3,2-d]pyrimidin-6-yl)propan-2-ol (3).** Compound 3 was prepared from 2-chloro-6-(4-methanesulfonyl-piperazin-1-ylmethyl)-4-morpholin-4-yl-thieno[3,2-d]pyrimidine<sup>8</sup> according to a similar Suzuki coupling procedure for compound 11. Mesylate salt <sup>1</sup>H NMR (400 MHz, DMSO) δ 8.66 (s, 1H), 8.30 (d, *J* = 8.0 Hz, 1H), 7.82 (d, *J* = 8.8 Hz, 1H), 7.58 (dd, *J* = 8.8, 8.0 Hz, 1H), 7.42 (s, 1H), 4.14 (m, 4H), 3.86 (m, 4H), 2.33 (s, 3H), 1.63 (s, 6H). MS (ESI): *m/z* (M + H)<sup>+</sup> 396. Analytical LC-MS on an Agilent (1100/MSD) using a 3 mm × 100 mm SD-C18 analytical column and H<sub>2</sub>O/MeCN modified with 0.05% trifluoroacetic acid running a linear gradient from 5% MeCN to 95% MeCN monitored by UV wavelength 254 nm and ESI+ TIC MS showed 99% purity.

**5-(6-((4-(Methylsulfonyl)piperazin-1-yl)methyl)-4-morpholinothieno[3,2-d]pyrimidin-2-yl)pyrimidin-2-amine (4).** Compound 4 was prepared from 2-chloro-6-(4-methanesulfonyl-piperazin-1-ylmethyl)-4-morpholin-4-yl-thieno[3,2-d]pyrimidine<sup>8</sup> according to a similar Suzuki coupling procedure for compound 11, using 5-(4,4,5,5-tetramethyl-1,3,2-dioxaborolan-2-yl)pyrimidin-2-amine. (41 mg, 57%). <sup>1</sup>H NMR (500 MHz, DMSO) δ 9.11 (s, 2H), 7.34 (s, 1H), 7.10 (s, 2H), 3.95–3.91 (m, 4H), 3.90 (s, 2H), 3.84–3.73 (m, 4H), 3.20–3.07 (m, 4H), 2.91 (s, 3H), 2.63–2.54 (m, 4H). <sup>13</sup>C NMR (126 MHz, DMSO) δ 164.04, 162.99, 161.92, 157.77,

157.25, 156.88, 150.01, 123.06, 120.04, 111.55, 65.97, 56.09, 51.78, 45.80, 45.34, 33.76. MS (ESI): *m/z* (M + H)<sup>+</sup> 491. Analytical LC-MS on an Agilent (1100/MSD) using a 3 mm × 100 mm SD-C18 analytical column and H<sub>2</sub>O/MeCN modified with 0.05% trifluoroacetic acid running a linear gradient from 5% MeCN to 95% MeCN monitored by UV wavelength 254 nm and ESI+ TIC MS showed 100% purity.

**(2-Chloro-4-morpholinothieno[3,2-d]pyrimidin-6-yl)methanol (9).** A solution of 4-morpholin-4-yl-2-[3-(1,1,2,2-tetramethyl-propylsilyloxy)-phenyl]-thieno[3,2-d]pyrimidine-6-carbaldehyde **7**<sup>8</sup> (0.2 g, 0.7 mmol) in MeOH (10 mL) at 0 °C was treated with sodium borohydride (0.1 g, 6 mmol). The solution was allowed to warm to room temperature and stirred for 15 min. The reaction mixture was quenched with water and extracted with ethyl acetate. The organic layer was dried with magnesium sulfate, filtered via Buchner funnel, and concentrated in vacuo to dryness. Crude yield = 100%. <sup>1</sup>H NMR (500 MHz, DMSO) δ 7.23 (s, 1H), 5.94 (t, *J* = 5.6 Hz, 1H), 4.82 (d, *J* = 4.9 Hz, 2H), 4.01–3.83 (m, 4H), 3.83–3.60 (m, 4H). MS (ESI): *m/z* (M + H)<sup>+</sup> 286.1. Analytical LC-MS on an Agilent (1100/MSD) using a 3 mm × 100 mm SD-C18 analytical column and H<sub>2</sub>O/MeCN modified with 0.05% trifluoroacetic acid running a linear gradient from 5% MeCN to 95% MeCN monitored by UV wavelength 254 nm and ESI+ TIC MS showed 100% purity.

**1-(2-(1H-Indazol-4-yl)-4-morpholinothieno[3,2-d]pyrimidin-6-yl)ethanol (18).** Compound 18 was prepared from 1-(2-chloro-4-morpholinothieno[3,2-d]pyrimidin-6-yl)ethanol (167 mg, 5.6 mmol) according to a similar Suzuki coupling procedure as described for compound 11, using 4-(4,4,5,5-tetramethyl-1,3,2-dioxaborolan-2-yl)-1H indazole and purified via reverse phase HPLC. Yield = 20%. <sup>1</sup>H NMR (500 MHz, DMSO) δ 13.17 (s, 1H), 8.90 (s, 1H), 8.24 (dd, *J* = 7.2 Hz, 0.6, 1H), 7.67 (d, *J* = 8.2 Hz, 1H), 7.53–7.46 (m, 1H), 7.43 (t, *J* = 3.4 Hz, 1H), 5.99 (d, *J* = 4.9 Hz, 1H), 5.15 (p, *J* = 5.5 Hz, 1H), 4.10–3.97 (m, 4H), 3.94–3.73 (m, 4H), 1.55 (d, *J* = 6.4 Hz, 3H). MS (ESI): *m/z* (M + H)<sup>+</sup> 382.1. Analytical LC-MS using Waters XBridge Phenyl analytical column and H<sub>2</sub>O/MeCN modified with 0.1% formic acid running a linear gradient from 5% MeCN to 95% MeCN monitored by UV wavelength 210 nm and ESI+ TIC MS showed 100% purity.

**2-[2-(2-Amino-4-methyl-pyrimidin-5-yl)-4-morpholin-4-yl-thieno[3,2-d]pyrimidin-6-yl]-propan-2-ol (19).** Compound 19 was prepared from 1-(2-chloro-4-morpholinothieno[3,2-d]pyrimidin-6-yl)ethanol (70 mg, 0.2 mmol) according to a similar Suzuki coupling procedure as described for compound 11, using 4-methyl-5-(4,4,5,5-tetramethyl-[1,3,2]dioxaborolan-2-yl)-pyrimidin-2-ylamine and purified via reverse phase HPLC. (15 mg, 20%) MS: 387.2 (M + H); <sup>1</sup>H NMR (400 MHz, DMSO) δ 8.84 (s, 1H), 7.42 (s, 1H), 4.08 (m, 4H), 3.81 (m, 4H), 1.61 (m, 9H). MS (ESI): *m/z* (M + H)<sup>+</sup> 387. Analytical LC-MS on an Agilent (1100/MSD) using a 3 mm × 100 mm SD-C18 analytical column and H<sub>2</sub>O/MeCN modified with 0.05% trifluoroacetic acid running a linear gradient from 5% MeCN to 95% MeCN monitored by UV wavelength 254 nm and ESI+ TIC MS showed 100% purity.

**5-[6-(4-Methanesulfonyl-piperazin-1-ylmethyl)-4-morpholin-4-yl-thieno[3,2-d]pyrimidin-2-yl]-4-methyl-pyrimidin-2-ylamine (20).** 2-Chloro-6-(4-methanesulfonyl-piperazin-1-ylmethyl)-4-morpholin-4-yl-thieno[3,2-d]pyrimidine (80 mg, 0.2 mmol), 4-methyl-5-(4,4,5,5-tetramethyl-[1,3,2]dioxaborolan-2-yl)-pyrimidin-2-ylamine (65 mg, 0.28 mmol), and bis(triphenylphosphine)palladium(II) dichloride (9.0 mg, 0.01 mmol) in 1 M aqueous sodium carbonate (0.8 mL) and acetonitrile (0.8 mL) were heated to 130 °C in a sealed microwave reactor for 15 min. Upon completion, the organic layer was separated and the aqueous layer was extracted with dichloromethane. The combined organic layers were concentrated in vacuo. The product was purified by reverse phase HPLC to yield 5-[6-(4-methanesulfonyl-piperazin-1-ylmethyl)-4-morpholin-4-yl-thieno[3,2-d]pyrimidin-2-yl]-4-methyl-pyrimidin-2-ylamine (10 mg, 10%). MS: 505.2 (M + H); <sup>1</sup>H NMR

(400 MHz, DMSO)  $\delta$  8.83 (s, 1H), 7.48 (s, 1H), 3.98 (m, 4H), 3.80 (m, 4H), 3.24 (m, 4H), 2.93 (m, 2H), 2.82 (m, 4H), 2.66 (m, 6H). MS (ESI):  $m/z$  ( $M + H$ )<sup>+</sup> 505. Analytical LC-MS on an Agilent (1100/MSD) using a 3 mm  $\times$  100 mm SD-C18 analytical column and H<sub>2</sub>O/MeCN modified with 0.05% trifluoroacetic acid running a linear gradient from 5% MeCN to 95% MeCN monitored by UV wavelength 254 nm and ESI+ TIC MS showed 100% purity.

**Synthesis of *N*-[2-(1*H*-Indazol-4-yl)-4-morpholin-4-yl-thieno[3,2-*d*]pyrimidin-6-ylmethyl]-acetamide (19).** 6-(Bromomethyl)-2-chloro-4-morpholinothieno[3,2-*d*]pyrimidine. To a solution of (2-chloro-4-morpholinothieno[3,2-*d*]pyrimidin-6-yl)methanol (100 mg, 0.4 mmol) in benzene (3.0 mL) at 0 °C was added PBr<sub>3</sub> (30  $\mu$ L, 0.4 mmol). The reaction was heated at reflux for 1 h. After cooling to room temperature, the reaction was quenched by the addition of water. The aqueous layer was extracted with EtOAc. The combined organics were dried over Na<sub>2</sub>SO<sub>4</sub> and concentrated in vacuo. The crude material was not purified further (115 mg). <sup>1</sup>H NMR (400 MHz, CDCl<sub>3</sub>)  $\delta$  7.32 (s, 1H), 4.71 (s, 2H), 3.99–3.97 (m, 4H), 3.85–3.83 (m, 4H). MS (ESI):  $m/z$  ( $M + H$ )<sup>+</sup> 347.9

**(2-Chloro-4-morpholinothieno[3,2-*d*]pyrimidin-6-yl)methanamine.** To a solution of 6-(bromomethyl)-2-chloro-4-morpholinothieno[3,2-*d*]pyrimidine (0.3 g, 0.9 mmol) in DMF (10 mL) was added K<sub>2</sub>CO<sub>3</sub> (0.2 g, 1.3 mmol), and phthalimide (0.1 g, 0.9 mmol). The resulting solution was stirred 20 h at room temperature. The reaction was concentrated in vacuo and diluted with water (10 mL). The heterogeneous mixture was filtered and the solid intermediate was carried onto the next step without purification. MS (ESI):  $m/z$  ( $M + H$ )<sup>+</sup> 415. To the solid phthalimide intermediate (100 mg, 0.24 mmol) in MeOH (7 mL) was added H<sub>2</sub>NNH<sub>2</sub>·H<sub>2</sub>O (24  $\mu$ L, 0.48 mmol). The reaction was heated 1 h at reflux. After cooling to room temperature, the reaction was quenched with water (10 mL) and extracted with EtOAc. The combined organics were dried over Na<sub>2</sub>SO<sub>4</sub> and concentrated in vacuo to afford (2-chloro-4-morpholinothieno[3,2-*d*]pyrimidin-6-yl)methanamine (0.05 g). <sup>1</sup>H NMR (400 MHz, CDCl<sub>3</sub>)  $\delta$  7.15 (s, 1H), 4.20 (s, 2H), 4.00–3.96 (m, 4H), 3.84–3.82 (m, 4H). MS (ESI):  $m/z$  ( $M + H$ )<sup>+</sup> 285.1

***N*-((2-Chloro-4-morpholinothieno[3,2-*d*]pyrimidin-6-yl)methyl)-acetamide.** To a solution of 4-morpholinothieno[3,2-*d*]pyrimidin-6-yl)methanamine (50 mg, 0.2 mmol) in CH<sub>2</sub>Cl<sub>2</sub> (4 mL) was added Et<sub>3</sub>N (84  $\mu$ L, 0.6 mmol) and acetyl chloride (0.3 mmol). The reaction was stirred overnight at room temperature before being quenched with water. The aqueous layer was extracted with EtOAc. The combined organics were dried over Na<sub>2</sub>SO<sub>4</sub> and concentrated in vacuo and used in the next step without purification. <sup>1</sup>H NMR (400 MHz, CDCl<sub>3</sub>)  $\delta$  7.17 (s, 1H), 4.68 (d,  $J$  = 6.1 Hz, 2H), 3.98–3.95 (m, 4H), 3.84–3.81 (m, 4H), 2.07 (s, 3H). MS (ESI):  $m/z$  ( $M + H$ )<sup>+</sup> 327.

***N*-[2-(1*H*-Indazol-4-yl)-4-morpholin-4-yl-thieno[3,2-*d*]pyrimidin-6-ylmethyl]-acetamide (19).** Compound 19 was prepared from *N*-((2-chloro-4-morpholinothieno[3,2-*d*]pyrimidin-6-yl)methyl)-acetamide according a similar Suzuki coupling procedure as described above for 16, using 4-(4,4,5,5-tetramethyl-1,3,2-dioxaborolan-2-yl)-1*H*-indazole. (41 mg from 50 mg of 4-morpholinothieno[3,2-*d*]pyrimidin-6-yl)methanamine). <sup>1</sup>H NMR (500 MHz, CDCl<sub>3</sub>)  $\delta$  9.00 (s, 1H), 8.27 (d,  $J$  = 7.1 Hz, 1H), 7.60 (d,  $J$  = 8.3 Hz, 1H), 7.53–7.47 (m, 2H), 4.76 (d,  $J$  = 5.9 Hz, 2H), 4.09–4.07 (m, 4H), 3.92–3.90 (m, 4H), 2.62 (s, 1H), 2.10 (s, 3H), 3.90 (s, 2H), 3.84–3.73 (m, 4H), 3.20–3.07 (m, 4H), 2.91 (s, 3H), 2.63–2.54 (m, 4H). MS (ESI):  $m/z$  ( $M + H$ )<sup>+</sup> 409.1.

**2-(2-(2-Amino-4-methylpyrimidin-5-yl)-4-morpholinothieno[3,2-*d*]pyrimidin-6-yl)propan-2-ol (20).** To a solution of 2-(2-chloro-4-morpholinothieno[3,2-*d*]pyrimidin-6-yl)propan-2-ol (1.0 g) in acetonitrile (6 mL) and 1 M aq Na<sub>2</sub>CO<sub>3</sub> (6 mL) was added Pd(PPh<sub>3</sub>)<sub>4</sub> (180 mg) and the reaction mixture was heated 15 min in a microwave reactor (300 W) at 140 °C. The reaction mixture was concentrated in vacuo and the desired product was purified by silica gel chromatography (2–8% MeOH in DCM) followed by recrystallization from EtOAc to afford 20 (650 mg). <sup>1</sup>H NMR

(500 MHz, DMSO):  $\delta$  8.77 (s, 1H), 7.38 (br s, 2H), 7.29 (s, 1H), 4.01 (app t, 4H), 3.80 (app t, 4H), 2.64 (s, 3H), 1.60 (s, 6H). MS (ESI):  $m/z$  387.2 ( $M + H$ )<sup>+</sup>.

**Characterization of Biochemical and Cellular Activity In Vitro.** Enzymatic activity of the Class I PI3K isoforms was measured using a fluorescence polarization assay that monitors formation of the product 3,4,5-inositoltriphosphate molecule as it competes with fluorescently labeled PIP3 for binding to the GRP-1 pleckstrin homology domain protein. An increase in phosphatidyl inositol-3-phosphate product results in a decrease in fluorescence polarization signal as the labeled fluorophore is displaced from the GRP-1 protein binding site. Class I PI3K isoforms were purchased from Perkin-Elmer or were expressed and purified as heterodimeric recombinant proteins (ref original JACS PI3K paper). Tetramethylrhodamine-labeled PIP3 (TAMRA-PIP3), di-C8-PIP2, and PIP3 detection reagents were purchased from Echelon Biosciences. PI3K isoforms were assayed under initial rate conditions in the presence of 10 mM Tris (pH 7.5), 25  $\mu$ M ATP, 9.75  $\mu$ M PIP2, 5% glycerol, 4 mM MgCl<sub>2</sub>, 50 mM NaCl, 0.05% (v/v) Chaps, 1 mM dithiothreitol, 2% (v/v) DMSO at the following concentrations for each isoform: PI3K $\alpha$ , $\beta$  at 60 ng/mL; PI3K $\gamma$  at 8 ng/mL; PI3K $\delta$  at 45 ng/mL. After assay for 30 min at 25 °C, reactions were terminated with a final concentration of 9 mM EDTA, 4.5 nM TAMRA-PIP3, and 4.2  $\mu$ g/mL GRP-1 detector protein before reading fluorescence polarization on an Envision plate reader. IC50s were calculated from the fit of the dose–response curves to a 4-parameter equation.

Human recombinant mTOR(1360–2549) was expressed and purified from insect cells and assayed using a Lanthascreen fluorescence resonance energy transfer format from Invitrogen in which phosphorylation of recombinant green fluorescent protein (GFP)-4EBP1 is detected using a terbium-labeled antibody to phospho-threonine 37/46 of 4-EBP1. Reactions were initiated with ATP and conducted in the presence of 50 mM Hepes (pH 7.5), 0.25 nM mTOR, 400 nM GFP-4E-BP1, 8  $\mu$ M ATP, 0.01% (v/v) Tween 20, 10 mM MnCl<sub>2</sub>, 1 mM EGTA, 1 mM dithiothreitol, and 1% (v/v) DMSO. Assays were conducted under initial rate conditions at room temperature for 30 min before terminating the reaction and detecting product in the presence of 2 nM Tb-anti-p4E-BP1 antibody and 10 mM EDTA. Dose–response curves were fit to an equation for competitive tight-binding inhibition and apparent  $K_i$ 's were calculated using the determined  $K_m$  for ATP of 6.1  $\mu$ M.

Antiproliferative cellular assays were conducted using PC3 and MCF7.1 human tumor cell lines provided by the ATCC or Genentech Research laboratories, respectively. MCF7.1 is an *in vivo* selected line developed at Genentech and originally derived from the parental human MCF7 breast cancer cell line (ATCC, Manassas, VA). Cell lines were cultured in RPMI supplemented with 10% fetal bovine serum, 100 units/mL penicillin, and 100  $\mu$ g/mL streptomycin, 10 mM HEPES, and 2 mM glutamine at 37 °C under 5% CO<sub>2</sub>. MCF7.1 cells or PC3 cells were seeded in 384-well plates in media at 1000 cells/well or 3000 cells/well, respectively, and incubated overnight prior to the addition of compounds to a final DMSO concentration of 0.5% v/v. MCF7.1 cells and PC3 cells were incubated for 3 and 4 days, respectively, prior to the addition of CellTiter-Glo reagent (Promega) and reading of luminescence using an Analyst plate reader. For antiproliferative assays, a cytostatic agent such as aphidicolin and a cytotoxic agent such as staurosporine were included as controls. Dose–response curves were fit to a 4-parameter equation and relative IC50s were calculated using Assay Explorer software.

**In Vivo Xenograft Studies.** Human prostate cancer PC3 cells obtained from the National Cancer Institute (Frederick, MD) were resuspended in Hank's Balanced Salt Solution and 3  $\times$  10<sup>6</sup> cells implanted subcutaneously into the right hind flank of athymic nu/nu (nude) mice. Tumors were monitored until they reached a mean tumor volume of 150–200 mm<sup>3</sup> prior to the

initiation of dosing. MCF7.1 cells resuspended in a 1:1 mixture of Hank's Buffered Salt Solution and Matrigel Basement Membrane Matrix (No. 356237, BD Biosciences; Santa Cruz, CA), were  $5 \times 10^6$  subcutaneously implanted into the right hind flank of athymic nu/nu (nude) mice. Prior to cell inoculation, 17  $\beta$ -estradiol (0.36 mg/pellet, 60-day release, No. SE-121) obtained from Innovative Research of America (Sarasota, FL) were implanted into the dorsal shoulder blade area of each nude mouse. After implantation of cells, tumors were monitored until they reached a mean tumor volume of 250–350 mm<sup>3</sup> prior to initiating dosing. Compound **5** and **21** were dissolved in 0.5% methylcellulose with 0.2% Tween-80 (MCT). Female nude (nu/nu) mice that were 6–8 weeks old and weighed 20–30 g were obtained from Charles River Laboratories (Hollister, CA). Tumor bearing mice were dosed daily for 14 to 21 days depending on the xenograft model with 100  $\mu$ L of vehicle (MCT) or test agent orally.

Tumor volume was measured in two dimensions (length and width) using Ultra Cal-IV calipers (model 54-10-111; Fred V. Fowler Company; Newton, MA) and was analyzed using Excel version 11.2 (Microsoft Corporation; Redmond, WA). The tumor volume (mm<sup>3</sup>) = (longer measurement  $\times$  shorter measurement<sup>2</sup>)  $\times$  0.5. Animal body weights were measured using an Adventurer Pro AV812 scale (Ohaus Corporation; Pine Brook, NJ). Percent weight change =  $[1 - (\text{new weight} / \text{initial weight})] \times 100$ . Tumor sizes were recorded twice weekly over the course of the study (14–21 days). Mouse body weights were also recorded twice weekly and the mice were observed daily. Mice with tumor volumes  $\geq 2000$  mm<sup>3</sup> or with losses in body weight  $\geq 20\%$  from their initial body weight were promptly euthanized per IACUC guidelines. Mean tumor volume and SEM values ( $n = 10$ ) were calculated using JMP statistical software, version 5.1.2 at end of treatment. % Tumor inhibition =  $100(\text{mean volume of tumors in vehicle treated animals} - \text{mean volume of tumors in test article treated animals given the test article}) / \text{mean volume of tumors in vehicle treated animals}$ . Data were analyzed and  $p$ -values were determined using the Dunnett  $t$  test with JMP statistical software, version 5.1.2 (SAS Institute; Cary, NC).

**Pharmacodynamic Analysis of the PI3K/Akt Pathway in Vivo.** MCF7.1 tumors were excised from animals and immediately snap frozen in liquid nitrogen. Frozen tumors were weighed and lysed with a pestle PP (Scienceware; Pequannock, NJ) in cell extract buffer (Biosource; Carlsbad, CA) supplemented with protease inhibitors (F. Hoffman-LaRoche, Ltd.; Mannheim, Germany), 1 mM phenylmethanesulfonyl fluoride, and phosphatase inhibitor cocktails 1 and 2 (Sigma; St. Louis, MO). Protein concentrations were determined using the Pierce BCA Protein Assay Kit (Rockford, IL). Levels of pAkt (Ser<sup>473</sup>) and pS6RP(Ser<sup>235/236</sup>) were assessed using kits measuring electrochemiluminescence from Meso Scale Discovery (Gaithersburg, MD). Levels of pPras40 (Thr<sup>246</sup>) was determined using an ELISA measuring absorbance at 450 nm from Biosource (Carlsbad, CA).

**Acknowledgment.** The authors wish to thank Mengling Wong, Martin Struble, and Wen Chiu for compound purification and determination of purity by HPLC, mass spectroscopy, and <sup>1</sup>H NMR. We thank Krista K. Bowman, Alberto Estevez, Kyle Mortara, and Jiansheng Wu for technical assistance of protein expression and purification, and Jeremy Murray for depositing structures to the PDB. We thank Emil Plise for plasma protein binding data. We are grateful to Michelle Nannini, Janeko Bower, Alex Vanderbilt, Alfonso Arrazate, Judi-Anne Ramiscal, Vincent Javinal, and Kenton Wong for coordinating and dosing animals for the described efficacy studies.

## References

- (1) (a) Vivanco, I.; Sawyers, C. L. The phosphatidylinositol 3-kinase AKT pathway in human cancer. *Nat. Rev. Cancer* **2002**, *2*, 489–501. (b) Cantley, L. C. The phosphoinositide 3-kinase pathway. *Science* **2002**, *296*, 1655–1657.
- (2) Backer, J. M. The regulation and function of class III PI3Ks: novel roles for Vps34. *Biochem. J.* **2008**, *410*, 1–17.
- (3) (a) Guertin, D. A.; Sabatini, D. M. Defining the role of mTOR in cancer. *Cancer Cell* **2007**, *12*, 9–22. (b) Fasolo, A.; Sessa, C. mTOR inhibitors in the treatment of cancer. *Exp. Opin. Investig. Drugs* **2008**, *17*, 1717–1734.
- (4) Bellacosa, A.; Kumar, C. C.; Di Cristofano, A.; Testa, J. C. Activation of AKT kinases in cancer: implications for therapeutic targeting. *Adv. Cancer Res.* **2005**, *94*, 29–86.
- (5) (a) Shayesteh, L.; Kuo, W. L.; Baldocchi, R.; Godfrey, T.; Collins, C.; Pinkel, D.; Powell, B.; Mills, G. B.; Gray, J. W. PIK3CA is implicated as an oncogene in ovarian cancer. *Nat. Genet.* **1999**, *21*, 99–102. (b) Samuels, Y.; Wang, Z.; Bardelli, A.; Silliman, N.; Ptak, J.; Szabo, S.; Yan, H.; Gazdar, A.; Powell, S. M.; Riggins, G. J.; Willson, J. K.; Markowitz, S.; Kinzler, K. W.; Vogelstein, B.; Velculescu, V. E. High frequency of mutations of the PIK3CA gene in human cancers. *Science* **2004**, *30*, 554. (c) Parsons, D. W.; Wang, T. L.; Samuels, Y.; Bardelli, A.; Cummins, J. M.; DeLong, L.; Silliman, N.; Ptak, J.; Szabo, S.; Willson, J. K.; Markowitz, S.; Kinzler, K. W.; Vogelstein, B.; Lengauer, C.; Velculescu, V. E. Colorectal cancer: mutations in a signalling pathway. *Nature* **2005**, *436*, 792. (d) Sulis, M. L.; Parsons, R. PTEN: from pathology to biology. *Trends Cell. Biol.* **2003**, *13*, 478–483. (e) Li, J.; Yen, C.; Liaw, D.; Podsypanina, K.; Bose, S.; Wang, S. I.; Puc, J.; Miliareis, C.; Rodgers, L.; McCombie, R.; Bigner, S. H.; Giovannella, B. C.; Ittmann, M.; Tycko, B.; Hibshoosh, H.; Wigler, M. H.; Parsons, R. PTEN, a putative protein tyrosine phosphatase gene mutated in human brain, breast, and prostate cancer. *Science* **1997**, *275*, 1943–1947.
- (6) Ihle, N. T.; Powis, G. Take your PIK: phosphatidylinositol 3-kinase inhibitors race through the clinic and toward cancer therapy. *Mol. Cancer Ther.* **2009**, *8* (1), 1–9.
- (7) (a) Raynaud, F. I.; Eccles, S. A.; Patel, S.; Alix, S.; Box, G.; Chuckowree, I. S.; Folkes, A. J.; Gowan, S.; Brandon, A. D. H.; Stefano, F. D.; Hayes, A.; Henley, A. T.; Lensun, L.; Pergl-Wilson, G. H.; Robson, A.; Saghir, N.; Zhyvoloup, P.; McDonald, E.; Sheldrake, P.; Shuttleworth, S.; Valenti, M.; Wan, N. C.; Clarke, P. A.; Workman, P. Biological properties of potent inhibitors of class I phosphatidylinositol 3-kinase: from PI-103 through PI-540, PI-620 to the oral agent GDC-0941. *Mol. Cancer Ther.* **2009**, *8* (7), 1725–1738. (b) Maria, S.-M.; Stauffer, F.; Brueggen, J.; Furet, P.; Schnell, C.; Fritsch, C.; Brachmann, S.; Chene, P.; De Pover, A.; Schoemaker, K.; Fabbro, D.; Gabriel, D.; Simonen, M.; Murphy, L.; Finan, P.; Sellers, W.; Garcia-Echeverria, C. Identification and characterization of NVP-BEZ235 a new orally available dual phosphatidylinositol 3-kinase/mammalian target of rapamycin inhibitor with potent in vivo antitumor activity. *Mol. Cancer Ther.* **2008**, *7* (7), 1851–1863.
- (8) Folkes, A. J.; Ahmadi, K.; Alderton, W. K.; Alix, S.; Baker, S. J.; Box, G.; Chuckowree, I. S.; Clarke, P. A.; Depledge, P.; Eccles, S. A.; Friedman, L. S.; Hayes, A.; Hancox, T. C.; Kugendradas, A.; Lensun, L.; Moore, P.; Olivero, A. G.; Pang, J.; Patel, S.; Pergl-Wilson, G. H.; Raynaud, F. I.; Robson, A.; Saghir, N.; Salphati, L.; Sohal, S.; Ultsch, M. H.; Valenti, M.; Wallweber, H. J. A.; Wan, N. C.; Wiesmann, C.; Workman, P.; Zhyvoloup, P.; Zvelebil, M. J.; Shuttleworth, S. J. The identification of 2-(1H-Indazol-4-yl)-6-(4-methanesulfonyl-piperazin-1-ylmethyl)-4-morpholin-4-yl-thieno-[3,2-d]pyrimidine (GDC-0941) as a potent, selective, orally bioavailable inhibitor of class I PI3 kinase for the treatment of cancer. *J. Med. Chem.* **2008**, *51*, 5522–5532.
- (9) This critical interaction with the enzyme was noted for molecules in 2 other series: (a) Vlahos, C. J.; Matter, W. F.; Hui, K. Y.; Brown, R. F. A specific inhibitor of phosphatidylinositol 3-kinase, 2-(4-morpholinyl)-8-phenyl-4H-1-benzopyran-4-one (LY294002). *J. Biol. Chem.* **1994**, *269*, 5241–5248. (b) Hayakawa, M.; Kaizawa, H.; Moritomo, H.; Koizumi, T.; Ohishi, T.; Okada, M.; Ohta, M.; Tsukamoto, S.; Parker, P.; Workman, P.; Waterfield, M. Synthesis and biological evaluation of 4-morpholino-2-phenylquinazolines and related derivatives as novel PI3 kinase PI3KR inhibitors. *Biorg. Med. Chem.* **2006**, *14*, 6847–6858.
- (10) Borwell, F. G. Equilibrium acidities in dimethyl sulfoxide solution. *Acc. Chem. Res.* **1988**, *21*, 456–463.
- (11) Obach, R. S.; Baxter, J. G.; Liston, T. E.; Silber, B. M.; Jones, B. C.; MacIntyre, F.; Rance, D. J.; Wastall, P. The prediction of human pharmacokinetic parameters from preclinical and in vitro metabolism data. *J. Pharmacol. Exp. Ther.* **1997**, *283*, 46–58.